ISSN 0006-2979, Biochemistry (Moscow), 2012, Vol. 77, No. 5, pp. 444-455. © Pleiades Publishing, Ltd., 2012.
Published in Russian in Biokhimiya, 2012, Vol. 77, No. 5, pp. 555-567.
Originally published in Biochemistry (Moscow) On-Line Papers in Press, as Manuscript BM12-009, March 4, 2012.

Femtosecond Charge Separation in Dry Films of Reaction Centers of *Rhodobacter sphaeroides* and *Chloroflexus aurantiacus*

A. G. Yakovlev[1]*, A. Yu. Khmelnitsky[2], and V. A. Shuvalov[1,2]

[1]*Department of Photobiophysics, Belozersky Institute of Chemical and Physical Biology, Lomonosov Moscow State University, 119991 Moscow, Russia; fax: (495) 939-3181; E-mail: yakov@genebee.msu.su*
[2]*Institute of Basic Biological Problems, Russian Academy of Sciences, 142290 Pushchino, Moscow Region, Russia; fax: (496) 773-0532; E-mail: shuvalov@issp.serpukhov.su*

Received January 12, 2012
Revision received January 30, 2012

Abstract—In this work, the influence of the crystallographic water on electron transfer between primary donor P and acceptor B_A was studied in reaction centers (RCs) of the purple bacterium *Rhodobacter sphaeroides* and the green bacterium *Chloroflexus aurantiacus*. For this purpose, time constants and oscillations of charge separation kinetics are compared between dry film RCs and RCs in glycerol–water buffer at 90 K. A common result of the drying of *Rba. sphaeroides* and *Cfx. aurantiacus* RCs is slowing of the charge separation process, decrease in amplitude of the oscillatory components of the kinetics, and the depletion of its spectrum. Thus, the major time constant of stimulated emission decay of P* bacteriochlorophyll dimer at 940 nm is increased from 1.1 psec for water-containing *Rba. sphaeroides* RCs to 1.9 psec for dry films of *Rba. sphaeroides* RCs. An analogous increase from 3.5 to 4.2 psec takes place in *Cfx. aurantiacus* RCs. In dry films of *Rba. sphaeroides* RCs, the amplitude of coherent oscillations of the absorption band of monomeric bacteriochlorophyll B_A^- at 1020 nm is 1.8 times less for the 130-cm^{-1} component and 2.3 times less for the 32-cm^{-1} component than the analogous amplitudes for water-containing RCs. Measurements in the analogous band of *Cfx. aurantiacus* RCs show that strong decrease (~5-10 times) of the B_A^- absorption band and strong slowing (from ~0.8 to ~3 psec) of B_A^- accumulation together with ~3-fold decrease in oscillation amplitude occurs on drying of these RCs. The overtones of the 32-cm^{-1} component disappeared from the oscillations of the kinetics at 940 and 1020-1028 nm after drying of the *Rba. sphaeroides* and *Cfx. aurantiacus* RCs. The results are in agreement with the results for GM203L mutant of *Rba. sphaeroides*, in which the HOH55 water molecule is sterically removed, and with the results for dry films of pheophytin-modified RCs of *Rba. sphaeroides* R-26 and for YM210W and YM210L *Rba. sphaeroides* mutant RCs. The data are discussed in terms of the influence (or participation) of the HOH55 water molecule on electron transfer along the chain of polar atomic groups N-Mg(P_B)-N-C-N(HisM202)-HOH55-O=(B_A) connecting P_B and B_A in *Rba. sphaeroides* RCs.

DOI: 10.1134/S0006297912050045

Key words: photosynthesis, charge separation, reaction center, wave packet, electron transfer

Reaction center (RC) of bacterial photosynthesis is a pigment–protein complex that is a part of photosynthetic membrane in which light energy is converted into chemical energy of charge separated states as a result of series of fast electron transfer reactions. The three-dimensional structure of RCs of the purple bacteria *Blastochloris* (*Rhodopseudomonas*) *viridis* and *Rhodobacter* (*Rba.*) *sphaeroides* has been studied by X-ray structure analysis [1, 2]. The RCs of *Rba. sphaeroides* consist of three protein subunits with different mass noted as H (heavy), L (light), and M (middle) and a number of cofactors embedded into the L and M subunits. These cofactors form two symmetric branches noted as A and B. Both branches spring from two common bacteriochlorophyll (BChl) molecules, P_A and P_B, which form the primary electron donor, dimer P that is placed near the periplasmic side of the membrane. Each of the branches proceeds further with a monomeric BChl molecule (B_A or B_B), a bacteriopheophytin (BPheo) molecule (H_A or

Abbreviations: ΔA, absorbance change (light-minus-dark); BChl, bacteriochlorophyll; B_A and B_B, monomeric BChl in A- and B-branch, respectively; BPheo, bacteriopheophytin; H_A and H_B, BPheo in A- and B-branch, respectively; P, primary electron donor, dimer BChl; P_A and P_B, BChl molecules constituting P; Q_A and Q_B, primary and secondary quinone, respectively; RC, reaction center; *Cfx.*, *Chloroflexus*; *Rba.*, *Rhodobacter*.

* To whom correspondence should be addressed.

H_B), and a quinone molecule (Q_A or Q_B) that is placed at the end of the branch near the cytoplasmic side of the membrane. An atom of nonheme iron and a carotenoid molecule are also included in the composition of the RC. Only the A-branch is photochemically active. On excitation of P, an electron is transferred from the first singlet excited level of P* to B_A within ~3 psec at room temperature, forming the first charge-separated state $P^+B_A^-$ [3-14]. Then the electron passes from B_A^- to H_A within ~1 psec at room temperature, forming the state $P^+H_A^-$. The fact that the state $P^+B_A^-$ is depleted several times faster than it is populated leads to significant problems in its detection. It is possible to detect it by registration of the BChl anion absorption band at 1020 nm [7, 8, 12, 15]. Next step is the electron transfer from H_A^- to Q_A within ~200 psec at room temperature with formation of the $P^+Q_A^-$ state. All the reactions are 2-3 times accelerated at cryogenic temperatures. The quantum yield of the whole process is close to 1 both at room and low temperatures [16-18]. Each further step of electron transfer is accompanied by free energy loss in exchange with increase of dissipation time of stored energy from ~300 psec for the P* state to ~0.1 sec for the $P^+Q_A^-$ state. The electron departs from the P^+ cation in each further stage: the distances between the P and B_A, P and H_A, and P and Q_A molecule centers are 11, 16, and 25 Å, respectively [1, 2].

Beside the above cofactors, the crystallographic water molecule HOH55 placed between P_B and B_A is also included into the structure of *Rba. sphaeroides* RCs (file 1AIJ from Protein Data Bank and Fig. 1) [19, 20]. The symmetrically located molecule HOH30 is in the B-branch of the RC. Water HOH55 is within the distance of H-bond creation both from oxygen of the 13^1-ketocarbonyl group of B_A and nitrogen of the His M202 residue that provides axial liganding of the central atom of magnesium in the BChl P_B [19-21]. Thus, there is a direct spacial connection between P_B and B_A through HOH55 and His M202.

The RC from the thermophilic green bacterium *Chloroflexus* (*Cfx.*) *aurantiacus* consists of three BChl molecules, three BPheo molecules, two molecules of menaquinone Q_A and Q_B, and a manganese atom [22-29]. A large amount of data on polypeptide structure, spectroscopy, and calculations of excitonic interaction indicates that the cofactors of *Cfx. aurantiacus* RC form two pigment branches as in *Rba. sphaeroides* RC [30-37]. Dimeric BChl is the primary electron donor in *Cfx. aurantiacus* RC [22-29]. The photochemically active A-branch contains an accessory molecule of BChl B_A, molecule of BPheo H_A as intermediate electron acceptor, and molecule of Q_A. The B-branch of *Cfx. aurantiacus* RC contains two BPheo molecules, Φ_B and H_B, and a Q_B molecule, and also Φ_B is located in the B_B binding site [26, 38]. The three-dimensional structure of this RC is not yet known. Decay of the P* excited state of *Cfx. aurantiacus* RCs occurs with 7 psec time constant at 296 K, while two components of this decay with 2 and 24 psec time constants are

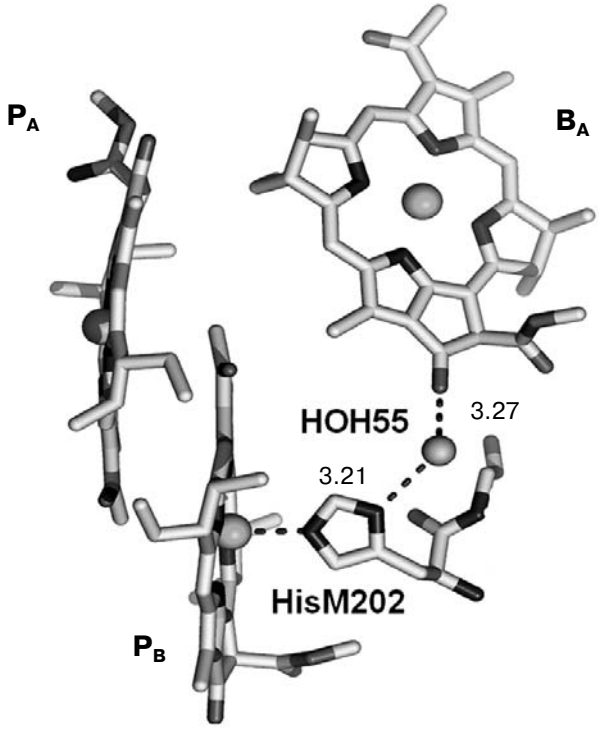

Fig. 1. A fragment of the three-dimensional structure of *Rba. sphaeroides* RCs according to Protein Data Bank (file 1AIJ). The BChl molecules P_A and P_B forming the dimer P, the molecule of accessory BChl B_A, the molecule of crystallographic water HOH55, and histidine M202 are shown. The phytol side chains of the BChl are not shown for simplicity. Hydrogen bonds are shown by dashed lines. Numbers are distances in Å. There is the direct space connection between P and B_A through the chain of atoms N-Mg(P_B)-N-C-N(HisM202)-HOH55-O=(B_A).

resolved at 10 K [39, 40]. The quantum yield of primary charge separation at 280 K [41] and room temperature [42] is close to 1. Electron transfer from H_A^- to the primary quinone Q_A occurs with ~320 psec time constant in *Cfx. aurantiacus* RCs at 280 K [25]. In spite of similarity to purple bacteria RCs in chromophore arrangement and photochemistry, *Cfx. aurantiacus* RCs have a number of significant differences in protein and cofactor composition [22]. For example, Tyr M210 is replaced by Leu in *Cfx. aurantiacus* RCs, which could explain the slowing of the primary charge separation reaction.

Coherent optical spectroscopy with femtosecond temporal resolution permits study of nuclear motions of cofactors and protein that can cause or accompany the electron transfer reactions. Identification of coherent signals of vibrations or rotations of molecular groups bounded with redox chromophores and surrounding molecules can provide information on the possible paths of primary electron transfer. It was shown that excitation of P in purple bacteria RCs by ultrashort (<30 fsec) laser pulses with a broad spectrum leads to oscillations in the kinetics of the P* stimulated emission decay with frequencies in the range of 10-400 cm^{-1} [43-46]. The same oscillations were found

in spontaneous fluorescence of RCs [47]. These data were explained as being due to formation and coherent propagation of a nuclear wave packet along the potential energy surface of the P* excited state [44, 45, 48]. The P* stimulated emission band has short-wavelength (around 900 nm) and long-wavelength (930-940 nm) maxima because of the fact that the wave packet position on the potential energy surface depends on time and because of mutual displacement of the P* and P surfaces. The oscillations in the two maxima have opposite phases but the same frequencies. Coherent components were found in the kinetics of the charge-separated state $P^+B_A^-$ in *Rba. sphaeroides* R-26 RCs [49-53], that is in the kinetics of the B_A^- radical-anion absorption band at 1020 nm [15, 18, 50-53] and in the B_A bleaching kinetics at 800 nm [49, 54]. Coherent effects of the dynamics of $P^+H_A^-$ state formation were studied in *Rba. sphaeroides* RCs by measurements of periodic modulation in the kinetics of the Q_y absorption band bleaching at 760 nm [52, 53] and in the kinetics of electrochromic shift of BChl monomer [55]. Femtosecond oscillations of the kinetics of P* stimulated emission at 945 nm and of B_A^- absorption at 1028 nm were found in *Cfx. aurantiacus* RCs at 90 K [56]. In these RCs, kinetics at 1028 nm reflect a stabilization of the $P^+B_A^-$ state with characteristic time ~5 psec and the electron transfer to H_A within ~1 psec.

Fourier analysis of the oscillatory components of the accumulation kinetics of the $P^+B_A^-$ and $P^+H_A^-$ charge-separated states in the *Rba. sphaeroides* R-26 RCs revealed a dominant mode of the oscillations at 32 cm^{-1} and a progression of several (up to seven) bands with multiple of 32-cm^{-1} frequencies that were assumed to be the overtones of 32-cm^{-1} fundamental mode [53]. It was assumed that an activation of the 32-cm^{-1} mode is connected with a rotation of the HOH55 water molecule (Fig. 1). In the GM203L mutant of *Rba. sphaeroides*, change of Gly M203 to Leu leads to exclusion of the HOH55 water molecule without remarkable changes in the protein structure beyond the close vicinity of M203 [57]. Because of the lack of polarity of Leu, there is no influence of M203 amino acid residue ionization on the primary electron transfer reaction in RCs of this mutant. It was found that the exclusion of the HOH55 water molecule from the RC structure by the GM203L mutation is accompanied by disappearance of the 32 cm^{-1} band from the Fourier transformed spectra of the oscillations of the kinetics at 1020 nm (B_A^- anion absorption band) and 760 nm (H_A bleaching band) and leads to more than four-fold slowing of electron transfer from P* to B_A [58]. These data may indicate a disruption of the most effective electron transfer path along the chain of polar atoms N-Mg(P_B)-N-C-N(HisM202)-HOH55-O=(B_A) in the GM203L mutant. In FM197R/GM203D *Rba. sphaeroides* double mutant, one of the carboxyl oxygen molecule from the Asp residue substituting for Gly M203 occupies a part of the space belonging to the HOH55 water molecule in the wild-type RCs that leads to steric removal of this water molecule [59]. The same structural alteration is assumed to occur in the RCs of the GM203D single mutant [59]. It was found that the P* lifetime is almost three times longer in FM197R/GM203D double mutant than in wild-type RCs [60].

It was found that isotopic drop of the 32-cm^{-1} fundamental oscillation mode occurred in the kinetics of the $P^+B_A^-$ and $P^+H_A^-$ charge-separated states of deuterated *Rba. sphaeroides* R-26 RCs [18, 53, 56]. This effect is most pronounced in deuterated pheophytin-modified *Rba. sphaeroides* R-26 RCs, in which picosecond electron transfer to H_A is blocked by substituting BPheo with plant pheophytin, and an accumulation of $P^+B_A^-$ state takes place that gives an opportunity to study in detail the oscillations from the kinetics of this state [58]. A 1.4-1.6 coefficient of the isotopic shift obtained in these works is close to the calculated one if a possibility of partial deuteration HOH→DOH is taken into account. Significant (several times) decrease in 32-cm^{-1} oscillation amplitude from the 1020 nm kinetics of the $P^+B_A^-$ state accumulation occurs on drying of pheophytin-modified *Rba. sphaeroides* RCs [18, 53]. Together with this effect, the slowing of $P^+B_A^-$ accumulation and decrease in ~120-cm^{-1} oscillation amplitude is also observed in these kinetics. When drying the pheophytin-modified *Rba. sphaeroides* RCs, a narrowing of the 120-cm^{-1} oscillation band having mostly vibrational nature is observed in the kinetics of P* stimulated emission decay. In dry films of YM210W and YM210L mutant *Rba. sphaeroides* RCs, the 1020 nm B_A^- absorption band is not observed, and a remarkable decrease in the oscillation amplitude is observed in the P* stimulated emission band at 940 nm [56].

In the present work, an influence of crystallographic water on the electron transfer between primary donor P and acceptor B_A was studied in RCs from the purple bacterium *Rba. sphaeroides* and the green bacterium *Cfx. aurantiacus*. For this purpose, time constants and oscillations of the charge separation kinetics are compared for dry film RCs and glycerol–water buffer RCs at 90 K. The main result of the drying of *Rba. sphaeroides* and *Cfx. aurantiacus* RCs is a slowing of the charge separation process, a decrease in the oscillatory component amplitude, and a depletion of its spectrum. This result is consistent with earlier data on GM203L *Rba. sphaeroides* mutant with sterically removed HOH55 water [58] and on dry films of pheophytin-modified *Rba. sphaeroides* R-26 RCs and YM210W and YM210L *Rba. sphaeroides* RCs [18, 53, 56]. The results are discussed in terms of influence (or participation) of the HOH55 water molecule in electron transfer along the chain of polar atom groups N-Mg(P_B)-N-C-N(HisM202)-HOH55-O=(B_A).

MATERIALS AND METHODS

Rhodobacter sphaeroides and *Cfx. aurantiacus* RCs were isolated by treatment of membranes with LDAO fol-

lowed by chromatography on DEAE cellulose [61]. The RCs were suspended in 10 mM Tris-HCl (pH 8.0), 0.1% Triton X-100 buffer (TT buffer). Low-temperature measurements at 90 K were performed on samples containing 65% glycerol (v/v). Optical density of the samples was 0.5 at 860 nm at room temperature. To keep the state $PB_AH_AQ_A^-$, 5 mM sodium dithionite was added to the RC samples. Absorption spectra of non-excited samples were measured using a Shimadzu UV-1601 PC spectrophotometer.

Dry RC film was made by drying RC solution at room temperature and ~40% relative humidity and then keeping the film in vacuum for 2 days. Before measurements, the film was illuminated by microsecond laser pulses to remove the remaining water molecules. The absorption spectrum of the dry film of RCs was slightly different from those of humid film by ~3 nm blue shift of the Q_Y band of P, while the Q_Y band of B_A was not shifted.

Femtosecond absorption changes (light-minus-dark) were measured with a laser spectrometer consisting of a Tsunami Ti-sapphire mode-locked fsec laser with Millennia cw laser pumping (both from Spectra Physics, USA). The laser pulses were amplified in an 8-pass Ti-sapphire amplifier and were used for generation of continuum in water. Duration of exciting and probing pulses was kept below 20 fsec. A polychromator and optical multichannel analyzer (Oriel, France) were used for measurements of absorption change spectra at different delays. The frequency of the spectrometric measurements was 15 Hz. The wavelength of excitation was 870 nm. The delay between excitation and probing pulses was set with 1 fsec accuracy. Temporal dispersion was less than 30 fsec in the 940-1060-nm range.

Differential absorption spectra were a result of averaging over 7000-10,000 measurements at each delay. The sensitivity of the spectrometer was $(1\text{-}3)\cdot10^{-5}$ OD. The kinetics of absorption changes (ΔA) at 1020-1028 nm were plotted using the measured maxima of absorption bands with additional subtraction of broadband background. Polynomial non-oscillatory curves, which were found mathematically and then subtracted from the initial kinetics, were used for approximation of the experimental kinetics. Standard approximation by exponentials was used only for evaluation of characteristic times of various processes. The oscillatory parts of the kinetics remaining after the subtraction were analyzed by Fourier transformation for obtaining the frequency spectra of the oscillations. Non-oscillatory curves corresponded to minimal noise of the Fourier spectra and to minimal amplitude of the oscillations.

RESULTS

In Fig. 2, low-temperature (90 K) difference (light-minus-dark) absorption spectra of dry films of *Rba. sphaeroides* (a) and *Cfx. aurantiacus* (b) RCs are shown in IR range at various temporal delays after photoexcitation by 20 fsec pulses at 870 nm. The shape of ΔA spectra of dry films of both RC types did not differ from those of glycerol–water buffer RCs [53, 56]. This indicates that the drying of RCs does not exert a destructive influence on them. For wavelengths shorter than 1000 nm, a bleaching caused by the long-wavelength slope of the P* stimulated emission band dominated in the presented spectra. The absorption band with maximum at 1020 nm for *Rba. sphaeroides* RCs and at 1028 nm for *Cfx. aurantiacus* RCs is the absorption band of BChl anion B_A^- [53, 56]. The amplitude of the B_A^- band of *Cfx. aurantiacus* RCs is several times smaller than those of *Rba. sphaeroides* RCs over the whole range of delays 0-3 psec. The B_A^- absorption bands of both RC types oscillate as a whole when the delay is varied, but their form and spectral maximum remains unchanged. The difference between the first oscillation maximum at 117 fsec and the first minimum at 217 fsec is especially remarkable. These oscillations are shown further in Figs. 4 and 6 in more detail.

In Fig. 3a data are shown for the P* stimulated emission band at 940 nm of dry films of *Rba. sphaeroides* RCs. These data demonstrate a decay of P* stimulated emission due to charge separation. The non-oscillatory part of the glycerol–water buffer kinetics is well approximated by two exponentials with time constants of 1.1 psec (77%) and 10 psec (23%). Overall slowing of the kinetics occurred after drying of the RCs, and three exponentials with time constants of 1.1 psec (8%), 1.9 psec (74%), and 10 psec (18%) are distinguished in them. Thus, the characteristic time of charge separation is increased on average from 1.1 to 1.9 psec in dry films of *Rba. sphaeroides* RCs. The 1.1 psec component dominated in the kinetics of water-containing RCs but remains as small component in dry film RCs. The oscillations in the kinetics of dry film RCs are similar to the analogous oscillations of glycerol–water buffer RCs and have the form of intense vibrations with ~220 fsec period that are completely damped during 1.5 psec (Fig. 3b). These oscillations have mostly vibrational nature and may reflect motions of BChl molecules inside the dimer P [43-46]. A broad band centered at ~130 cm^{-1} dominates in the Fourier spectra of the oscillations from both kinetics (Fig. 3c). In dry film RCs, this band is somewhat narrower than in water RCs and has two maxima at 128 and 169 cm^{-1}. Note that the Fourier spectrum of the water RC oscillations contains a number of weak narrow bands separated by an interval of ~30-32 cm^{-1} in accordance with earlier data [53]. These bands are absent in the Fourier spectrum of the oscillations from the dry film RC kinetics.

In Fig. 4, the kinetics of ΔA at 1020 nm (a) and their mathematical analysis (b and c) are shown for dry films of *Rba. sphaeroides* RCs. The kinetics of ΔA at 1020 nm for dry films and water RCs are close to each other and reflect fast (within ~120 fsec) formation of the $P^+B_A^-$ state fol-

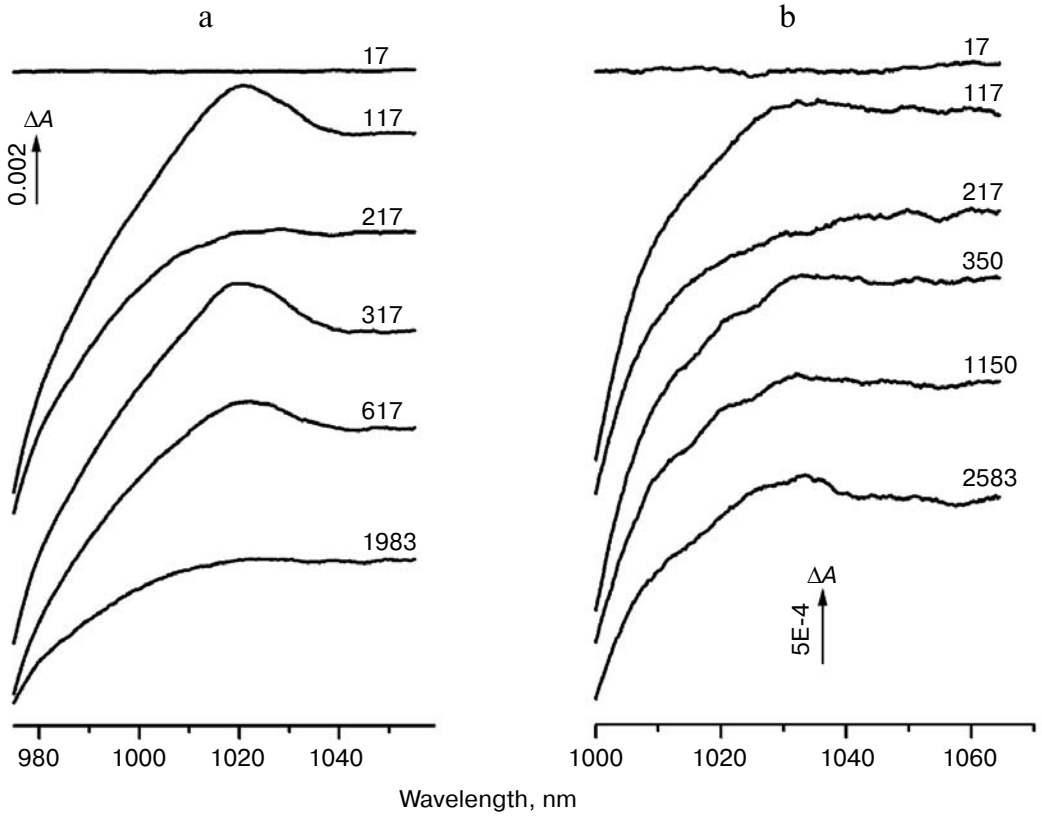

Fig. 2. Low-temperature (90 K) difference (light-minus-dark) absorption spectra of dry films of *Rba. sphaeroides* (a) and *Cfx. aurantiacus* (b) RCs at various temporal delays relative to the moment of the photoexcitation by 20-fsec pulses at 870 nm. Numbers are delays in femtoseconds. The amplitude of the absorption bands in their maximum at 1020 nm (a) and 1028 nm (b) was used for plotting the kinetics in Figs. 4 and 6 after subtracting the broadband background.

lowed by slower (within ~1.0-1.5 psec) decay of this state. This decay is somewhat slowed in dry film RCs in comparison with water RCs. The fast temporal component in the kinetics at 1020 nm corresponded to electron transfer to H_A, and the slow component to electron transfer from P* to B_A in accordance with the simple kinetic model of two-step electron transfer $P^* \rightarrow P^+B_A^- \rightarrow P^+H_A^-$. The presence of intense oscillations (almost 100% modulation during the first 0.5 psec) in the kinetics at 1020 nm (Fig. 4b) indicates predominant coherent processes in formation of the $P^+B_A^-$ state when a mixed state of P*, $P^+B_A^-$, and probably $P^+H_A^-$ is created [53]. These oscillations have initial period of ~220 fsec, like the oscillations in the kinetics at 940 nm (Fig. 3), and also they have a remarkable contribution of slower components with a period of ~1 psec. In dry film of RCs, the amplitude of the oscillations of the kinetics at 1020 nm is 1.8 times smaller for the component with 220-fsec period and 2.3 times smaller for the component with 1-psec period compared to the analogous amplitudes in water RCs. The Fourier spectrum of the oscillations at 1020 nm (Fig. 4c) has a complicated form and contains a narrow intense band at 32 cm^{-1}, narrow bands with multiple to 32-cm^{-1} frequencies (probably overtones), and broad band centered at ~130 cm^{-1}. In dry film RCs, the amplitude of the 32-cm^{-1} band from the Fourier spectrum of the oscillations is ~2-fold less than that in water-containing RCs. Besides, the amplitude of the overtones of the 32 cm^{-1} mode, especially of its second harmonic at 64-66 cm^{-1} is significantly decreased in the Fourier spectrum of the oscillations of dry film RCs.

In Fig. 5, the kinetics of ΔA of P* stimulated emission at 940 nm (a) and their mathematical analysis (b and c) are shown for dry film RCs of *Cfx. aurantiacus*. The decay of P* stimulated emission of the *Cfx. aurantiacus* RCs occur slower than that of *Rba. sphaeroides* (Fig. 3). The non-oscillatory part of the kinetics of ΔA of the *Cfx. aurantiacus* water RCs at 940 nm is adequately approximated by a sum of two exponentials with characteristic times of 3.5 psec (66%) and 20 psec (34%). The analogous approximation of the kinetics of dry film RCs produces the characteristic times of 4.2 psec (71%) and 20 psec (29%). Thus, slowing of the primary reaction of charge separation occurs on drying of the *Cfx. aurantiacus* RCs. The oscillations in the kinetics at 940 nm have initial period of ~220 fsec and are almost completely damped within ~1.5 psec (Fig. 5b). The amplitude of

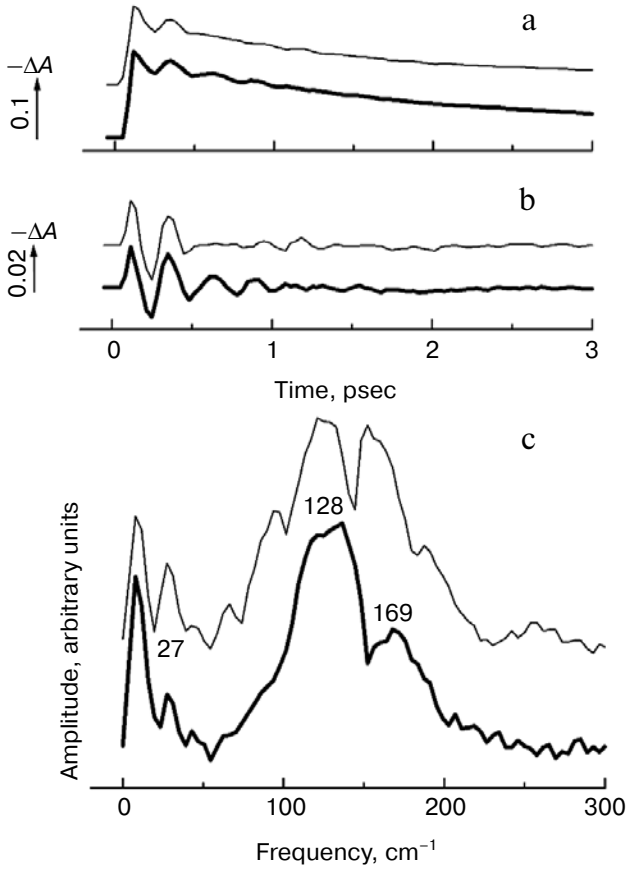

Fig. 3. Kinetics of ΔA at 940 nm (a), oscillatory components of these kinetics (b), and the Fourier-transformed spectrum of the oscillatory components (c) of dry films of *Rba. sphaeroides* RCs (thick lines) excited by 20-fsec pulses at 870 nm. The kinetics were measured at 90 K. The analogous data for *Rba. sphaeroides* RCs in glycerol–water buffer are shown by thin lines for comparison. Numbers in Fig. 3c are characteristic frequencies of the Fourier-transformed spectra.

these oscillations is slightly less (by ~15%) in the kinetics of dry film RCs than in the kinetics of water RCs. The Fourier spectrum of the kinetics of water RCs (Fig. 5c) contains a broad band with two maxima at ~113 and ~165 cm^{-1}. There are weak narrow bands in this spectrum also, most of which are approximately multiples of the 35-37 cm^{-1} band, as well as 37-cm^{-1} band itself. In the Fourier spectrum of the kinetics of dry film RCs, a narrowing of the main band by approximately 1.4-fold occurs in comparison with water-containing RCs. This band has two maxima at ~121 and ~157 cm^{-1} as well. Note that the bands with multiple of 35-37 cm^{-1} frequency are not observed in the Fourier spectrum of the kinetics of dry film RCs, but small narrow band at 37 cm^{-1} are present in this spectrum.

In Fig. 6, the kinetics of ΔA of the B_A^- absorption band at 1028 nm (a) and their mathematical analysis (b and c) are shown for dry films of the *Cfx. aurantiacus* RCs (thick lines). The kinetics of water RCs show an accumulation of B_A^- with characteristic time of ~0.8 psec during ~1 psec followed by an approximately constant part of the kinetics with extent of ~2 psec that is consistent with the data obtained earlier [56]. The oscillations in the kinetics of water RCs have complicated form: initial intensive vibrations with a period of ~200 fsec and distinct vibrations with lower frequency are resolved in them. The Fourier spectrum of the oscillations of water RCs contains narrow intense bands at 35 and 109 cm^{-1}, narrow bands of less intensity at 52 and 72 cm^{-1}, and a broad band at ~176 cm^{-1}. After drying of the *Cfx. aurantiacus* RCs, strong decrease by ~5-10-fold of the B_A^- absorption at 1028 nm occurred (Figs. 6a and 2). The kinetics of dry film RCs show gradual increase with time constant of ~3 psec during the whole range of measurement that is accompanied by oscillations. The amplitude of initial oscillations of the kinetics of dry film RCs with a period

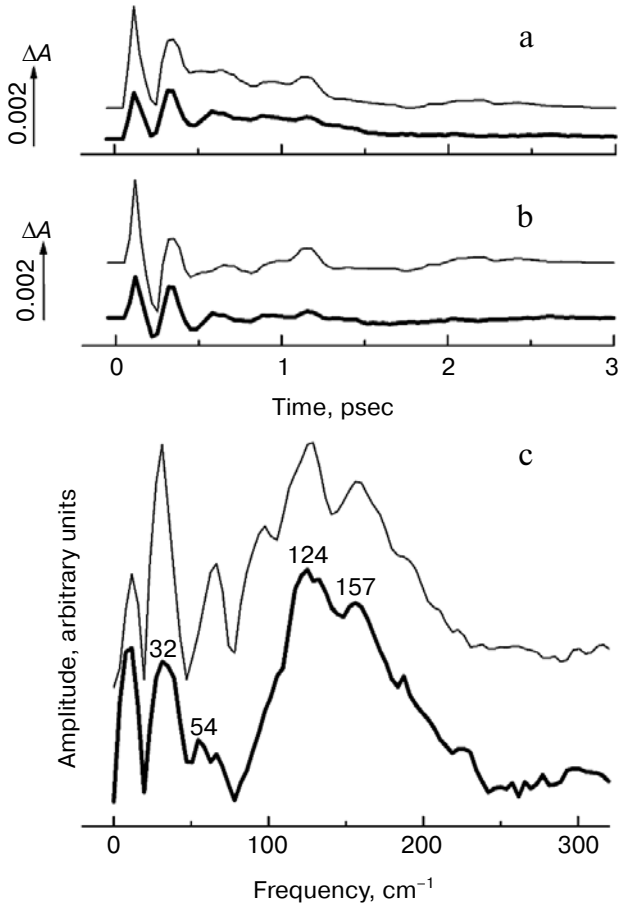

Fig. 4. Kinetics of ΔA at 1020 nm (a), oscillatory components of these kinetics (b), and the Fourier-transformed spectrum of oscillatory components (c) of dry films of *Rba. sphaeroides* RCs (thick lines) excited by 20-fsec pulses at 870 nm. The kinetics were measured at 90 K. The analogous data for *Rba. sphaeroides* RCs in glycerol–water buffer are shown by thin lines for comparison. Numbers in Fig. 4c are characteristic frequencies of the Fourier-transformed spectra.

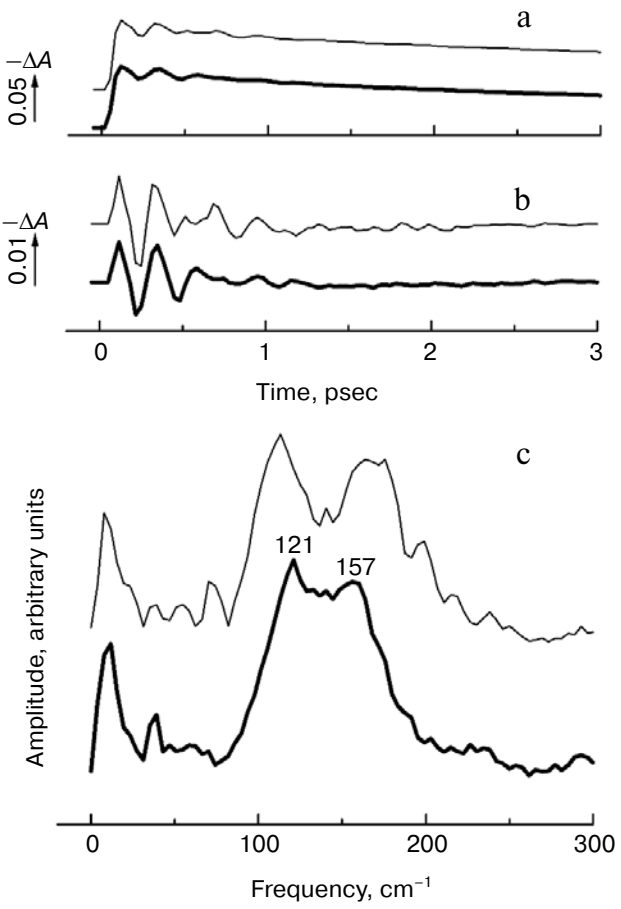

Fig. 5. Kinetics of ΔA at 940 nm (a), oscillatory components of these kinetics (b), and the Fourier-transformed spectrum of oscillatory components (c) of dry films of *Cfx. aurantiacus* RCs (thick lines) excited by 20-fsec pulses at 870 nm. The kinetics were measured at 90 K. The analogous data for *Cfx. aurantiacus* RCs in glycerol–water buffer are shown by thin lines for comparison. Numbers in Fig. 5c are characteristic frequencies of the Fourier-transformed spectra.

of ~200 fsec is decreased by ~3-fold in comparison with the water-containing RCs. Besides, the oscillations of the kinetics of dry film RCs do not contain low-frequency features around 2 psec observed in the oscillations of water RCs (Fig. 6b). The Fourier spectrum of the oscillations of dry film RCs contains weak bands at 37 and 90 cm^{-1}, and a band at ~160 cm^{-1} with strong noise.

In Fig. 7, Fourier transformed spectra of oscillatory parts of the kinetics of deuterated dry film *Rba. sphaeroides* RCs are shown for 940 nm (a) and 1020 nm (b). After deuteration of RCs, a drop of characteristic frequencies of the oscillations in the kinetics of P* stimulated emission at 940 nm and of B_A^- absorption at 1020 nm occurs in accordance with data obtained earlier (Figs. 3 and 4) [18, 53]. The coefficient of isotopic shift is varied within a range of 1.4-1.6 for different oscillation frequencies, which is close to its theoretical value if the probability of partial deuteration HOH→DOH is taken into account [53]. After drying of deuterated RCs, a narrowing and reverse shift to higher frequencies is observed for major band of the Fourier spectrum of the oscillations of the kinetics at 940 nm (Fig. 7a). This change is probably due to almost complete disappearance of several narrow bands with approximately multiple to 32 cm^{-1} frequencies, which are overlapped with the broad band at ~100 cm^{-1}, from the Fourier spectrum. In the Fourier spectrum of the oscillations of dry film deuterated RCs at 1020 nm, more than twofold decrease in the amplitudes of intense band at 23 cm^{-1} and multiple frequencies is observed together with a shift of the broad band at ~100 cm^{-1} to higher frequency (Fig. 7b). Thus, the spectra of the oscillations from the kinetics of dry film deuterated RCs are close to analogous spectra of dry films of non-deuterated RCs (Figs. 3 and 4).

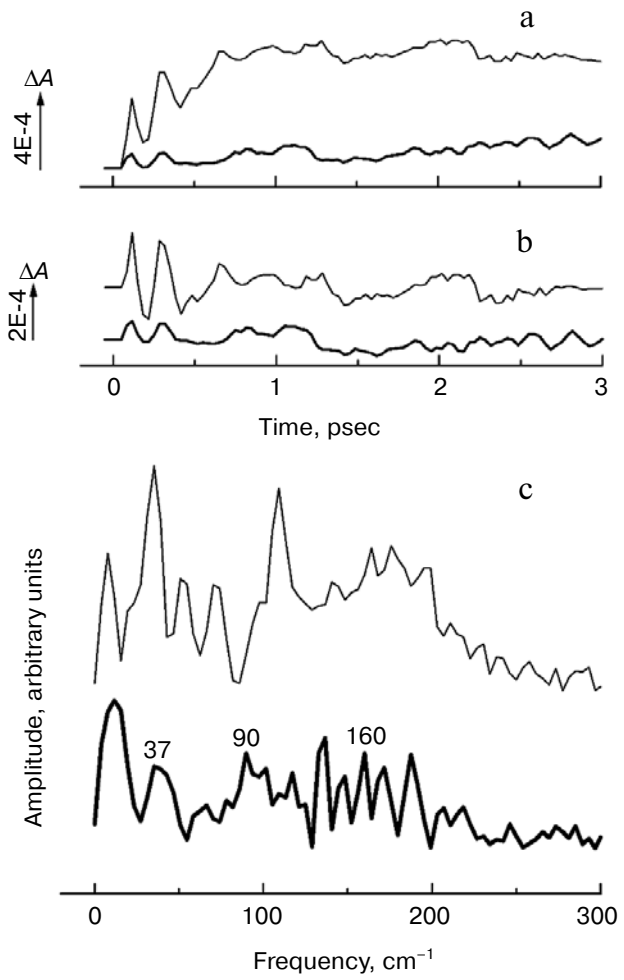

Fig. 6. Kinetics of ΔA at 1028 nm (a), oscillatory components of these kinetics (b), and the Fourier-transformed spectrum of oscillatory components (c) of dry films of *Cfx. aurantiacus* RCs (thick lines) excited by 20-fsec pulses at 870 nm. The kinetics were measured at 90 K. The analogous data for *Cfx. aurantiacus* RCs in glycerol–water buffer are shown by thin lines for comparison. Numbers in Fig. 6c are characteristic frequencies of the Fourier-transformed spectra.

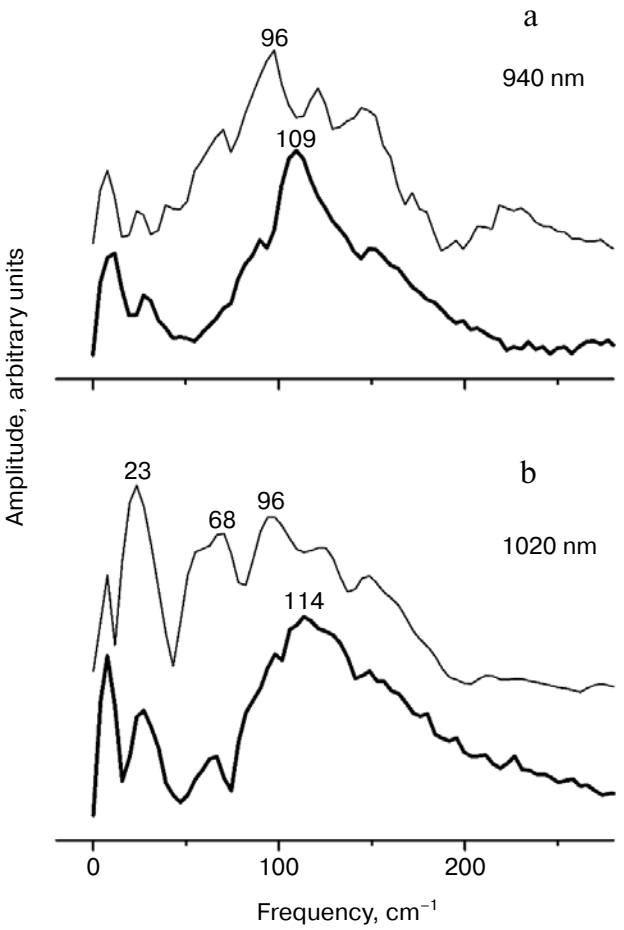

Fig. 7. Fourier-transformed spectrum of the oscillatory components of the kinetics of dry films of deuterated *Rba. sphaeroides* RCs (thick lines) at 940 nm (a) and 1020 nm (b) excited by 20-fsec pulses at 870 nm. The kinetics were measured at 90 K. The analogous data for *Rba. sphaeroides* RCs in glycerol/heavy water buffer are shown by thin lines for comparison. Numbers are characteristic frequencies of the Fourier-transformed spectra.

DISCUSSION

In this work, an influence of crystallographic water on electron transfer between the primary donor P and the acceptor B_A was studied in RCs of the purple bacterium *Rba. sphaeroides* and the green bacterium *Cfx. aurantiacus*. The main result of the drying of *Rba. sphaeroides* and *Cfx. aurantiacus* RCs is a slowing of the charge separation process, a decrease in the amplitude of the oscillatory components, and a rarefaction of its spectra. These results are consistent with earlier obtained results in GM203L *Rba. sphaeroides* mutant with sterically removed HOH55 water [58] and in dry films of pheophytin-modified *Rba. sphaeroides* R-26 RCs and YM210W and YM210L mutant *Rba. sphaeroides* RCs [18, 53]. In dry film RCs, the decay of P* stimulated emission is slowed by 1.7-fold (from 1.1 to 1.9 psec) in comparison with that for glycerol–water buffer RCs for *Rba. sphaeroides*, and by 1.2-fold (from 3.5 to 4.2 psec) for *Cfx. aurantiacus*. This is less than approximately twofold slowing of P* decay in the films of pheophytin-modified *Rba. sphaeroides* R-26 [18, 53] and fourfold slowing of P* decay in GM203L mutant *Rba. sphaeroides* RCs [58]. Perhaps, incomplete removal of water from RCs takes place during their drying. The 32 cm^{-1} mode and its overtones may be the rotation modes of water: they are presented in the Fourier spectrum of the oscillations in the kinetics of *Rba. sphaeroides* RCs but are absent in the analogous kinetics of GM203L *Rba. sphaeroides* mutant, where the HOH55 water molecule is absent [58]. A connection of this mode with rotation of the water molecule is also proved by its isotopic shift in deuterated *Rba. sphaeroides* RCs [18, 53, 58]. In *Cfx. aurantiacus* RCs, the 35-37 cm^{-1} mode is probably an analog of the 32 cm^{-1} mode. The three-dimensional structure of *Cfx. aurantiacus* RCs is not known yet, as well as the presence of crystallographic water HOH55 in these RCs. The decrease in the amplitude of these fundamental modes by ~2-fold in the Fourier spectrum of the oscillations as well as significant decrease in the amplitude of their overtones proves that these modes are related to the rotation of water. The fact that these modes are observed in the Fourier spectrum of the oscillations in dry films of RCs may point to partial exclusion of water from the RC films. The drying of RCs makes the most significant effect in the kinetics of the *Cfx. aurantiacus* B_A^- band that show strong decrease of this band and strong slowing of its formation (Fig. 6).

Let us consider possible explanations for the data. The first explanation is that the RCs contain several hundreds of non-crystallographic water molecules, some of them connected with protein subunits [62]. The exclusion of this water may leads to conformational changes in the protein environment of the cofactors and may influence the electron transfer reactions [63]. Probably, significant slowing of electron transfer to the secondary acceptor Q_B in dewatered RCs is explained by this [63]. Femtosecond spectroscopy data of primary charge separation reactions in the GM203L *Rba. sphaeroides* mutant show that the exclusion of the single molecule of crystallographic water HOH55 exerts more influence on these reactions than the removal (perhaps, partial) of all other water molecules on drying of RCs [58]. This fact shows the small influence of possible conformational protein changes on early steps of electron transfer in the dry RCs.

The second, more interesting explanation is that the HOH55 water molecule can be a part of the electron transfer chain consisting of the following polar atoms: N-Mg(P_B)-N-C-N(HisM202)-HOH55-O=(B_A) (Fig. 1). The HOH55 water molecule is located within distance of creation of hydrogen bonds from keto carbonyl group of B_A and from His M202, but the presence or absence of these bonds in early stages of charge separation needs further study. Resonance Raman scattering spectroscopy shows that the stretching frequency of B_A keto carbonyl is

1676 cm^{-1} in ferricyanide-oxidized wild-type RCs and 1704 cm^{-1} in GM203L mutant RCs. This means the presence of a relatively strong hydrogen bond between this group and HOH55 in the wild-type complex (4.1 kcal/mol [57]) and the absence of it in the GM203L mutant.

Damage to the completeness of the mentioned chain by the exclusion of the HOH55 water molecule in dry film RCs leads to disappearance of the fast component of electron transfer (1.1 psec in *Rba. sphaeroides* and 3.5 psec in *Cfx. aurantiacus*) due to an interruption of most probable route of electron tunneling. The slower components (1.9 and 10 psec in *Rba. sphaeroides*, 4.2 and 20 psec in *Cfx. aurantiacus*) may reflect other, less effective routes of electron transport probably belonging to nonspecific electron tunneling from P* to B_A. Direct electron tunneling through vacuum in the location of the extracted HOH55 water may be one of the possibilities too. Note that all of the routes of electron transfer from P* to B_A seems to be equally effective with respect to deactivation "P* $\rightarrow$ ground state", because the supposed quantum yield of $P^+B_A^-$ state is close to 100% if the time of pure deactivation of P* is equal to several hundreds of picoseconds [64-68].

According to quantum mechanical calculations [69], maximal density of electrons with π-spin in the P* state is located on the nitrogen atoms that are coordinated to the central Mg atom in the P_B molecule. This means that the Mg-liganding nitrogen atom of His M202 is also very close (~2 Å) to the area of maximal spin density of P_B. This is consistent with the assumption that the chain of polar groups mentioned above provides the main path of electron transfer with maximal speed. When this chain is broken because of the absence of HOH55, the speed of electron transport is several-fold decreased and this transport probably occurs along other ("nonspecific") paths of electron tunneling. It is necessary to note that the chain of polar groups that probably acts as a pipeline for electron transfer has a length that is greater than the shortest path of electron tunneling through space between P_A/P_B and B_A (~8.5 against 3.5-5.5 Å). The greater speed of electron transfer along this chain may be explained by the fact that the chain of polar group creates a medium that is more effective for electron tunneling than a vacuum, and the difference in the distances is compensated due to this fact. The path of electron tunneling along the bonds of this more extended chain may compete with the shorter path of vacuum tunneling because a hydrogen bond creates a medium that is approximately three times more effective for tunneling than vacuum [70].

Irrespective of the reason for the slowing of P* decay in RCs, it becomes clear from the Fourier analyses of the oscillatory components in Figs. 3-6 that the assumed rotation of water HOH55 following femtosecond excitation of the reaction center influences the dynamics of electron transfer from P* to B_A. The nature of HOH55 rotation is not clear at present. Also, it is not clear whether this rotation is necessary for maximal speed and yield of primary charge separation (see also [53]). Generally, rotation of a water molecule means the absence of hydrogen bonds with B_A and His M202 (Fig. 1) or a restoration of them after each revolution of the molecule. The latter seems improbable because the rotation energy of a single water molecule is insufficient to break hydrogen bonds again and to continue a rotation. Moreover, stochasticity of the rotation in space strongly decreases probability of exact restoration of molecular position that provides for creation of hydrogen bonds. On the other hand, the energy of ~300 cm^{-1} of the nuclear wave packet [53] is enough to break a hydrogen bond of ~1 kcal/mol strength. Coherent motion of the nuclear subsystem continuing after photoexcitation may provide energy that is enough for 2-3 revolutions of the HOH55 water molecule [18, 53]. The fact that only one of three fundamental frequencies of water rotation (20, 32, and 52 cm^{-1}) is presented in the oscillations of the RC kinetics needs to be explained as well. The rotation of a strong water dipole influences a transferred electron by Coulomb forces with a frequency of the rotation. This influence is clearly noticed in the kinetics of the B_A^- absorption band because the HOH55 water molecule is rather close to B_A. However, the frequencies that are close to water rotation frequencies and to their overtones are present in the kinetics of P* as well, which indicates the influence of the water rotation on P.

Another mechanism for the influence of water on electron transfer from P* to B_A is discussed in [57]. A decrease in the free energy level of the $P^+B_A^-$ state and its stabilization can occur when a hydrogen bond is created between the water and B_A. Based on the fact that strength of this hydrogen bond is maximal in oxidized RCs, it was assumed in [57] that an increase in positive charge on P due to separation of the electron occurs simultaneously with the decrease in $P^+B_A^-$ level caused by an increase in the strength of the hydrogen bond. As a result, the electron is dynamically stabilized on B_A during a short time that is approximately equal to the lifetime of this state (~1 psec). Perhaps this kind of stabilization of the $P^+B_A^-$ state is less inertial than the mechanism of reorientation of the OH-group of tyrosine M210 discussed in [53, 56]. Note that stabilization $P^+B_A^-$ is possible by reorientation of water HOH55 as well, because the time for this reorientation (~1-2 psec according to estimations from [62]) is comparable with the P* $\rightarrow$ $P^+B_A^-$ transition time.

Let us examine peculiarities of the B_A^- band kinetics in dry films of *Cfx. aurantiacus* RCs that show strong decrease in this band and strong slowing of its formation (Fig. 6) together with moderate slowing of P* stimulated emission decay (Fig. 5). A possible explanation for this discrepancy is that primary charge separation in *Cfx. aurantiacus* RCs can occur simultaneously along several channels [39]. Together with two-step transfer by scheme

$P^* \rightarrow P^+B_A^- \rightarrow P^+H_A^-$, a channel of direct transfer $P^* \rightarrow P^+H_A^-$ acts according to the quantum mechanism of superexchange with virtual participation of B_A as a mediator. In the latter case, the electron does not come to B_A, but energy levels of B_A are used virtually for electron transfer [71-77]. If it is assumed that direct transfer $P^* \rightarrow P^+H_A^-$ predominates in *Cfx. aurantiacus* RCs (which proceeds ~3-fold slower than the two-step transfer in *Rba. sphaeroides* RCs according to Fig. 5), then it becomes clear that the drying of these RCs blocks the minor two-step channel but does not affect the major one. Strong changes are observed in the B_A absorption band, and weak changes are observed in the P* emission band after this drying.

Let us examine details of stabilization of separated charges in dry films of RCs. We showed in previous studies that the time constant of reversible electron transfer from P* to B_A accompanied by light emission at 940 nm has a value less than 10-20 fsec [53, 56]. Based on this fact, one can assume that the speed of non-reversible electron transfer measured in experiment is determined by the process of charge stabilization in the pair of primary radicals $P^+B_A^-$. From this point of view, it is possible to examine two versions of charge stabilization [56]: 1) vibrational relaxation of the $P^+B_A^-$ state due to transfer of excessive energy to the bath; 2) reorientation of some surrounding groups, for example the OH-group of tyrosine M210, that accompanies the reversible formation of $P^+B_A^-$. The latter possibility is interesting for discussion because a substitution of tyrosine M210 by tryptophan or leucine leads to approximately 200-fold decrease in charge stabilization rate at low temperature ([56] and references in this work). It was assumed in the discussion of [56] that the reversible electron transfer from P* to B_A with a period of 260 fsec in native *Rba. sphaeroides* RCs is accompanied by stabilization of $P^+B_A^-$ due to the shift of $H^{\delta+}$ of the $O^{\delta-}H^{\delta+}$ dipole of tyrosine M210 towards B_A during four cycles of reversible electron transfer, that is within the time of ~1 psec at 90 K. This means that about 22% of the total amount of RCs stabilized in the state $P^+B_A^-$ after 4 psec is accumulated in each of the cycles. In dry films of *Rba. sphaeroides* RCs, the period of reversible electron transfer from P* to B_A is not significantly changed, but the amplitude of the oscillations at 1020 nm is decreased by several times in comparison with water buffer RCs (Fig. 4b). The analogous conclusion is correct for the dry films of *Cfx. aurantiacus* RCs as well (Fig. 6b), in which tyrosine M195 may participate in the charge stabilization [56]. These data may mean that the decrease in the amplitude of reversible electron transfer from P* to B_A may be referred to overall slowing of the stabilization of the $P^+B_A^-$ state. Nevertheless, additional investigations of this problem are needed.

In conclusion, the present results give clear evidence that the molecule of crystallographic water HOH55 has a strong influence on primary charge separation in *Rba. sphaeroides* RCs, or directly participates in this process. In *Cfx. aurantiacus* RCs, the data proves the assumption that an analog of the HOH55 molecule (or molecules) is present in these RCs and plays the same role as the HOH55 molecule in *Rba. sphaeroides* RCs. The mentioned influence/participation permits understanding of the details of the primary stage of the charge separation process.

This work was done with financial support of the Russian Foundation for Basic Research (grant No. 11-04-00312).

REFERENCES

1. Deisenhofer, J., Epp, O., Miki, K., Huber, R., and Michel, H. (1984) *J. Mol. Biol.*, **180**, 385-398.
2. Allen, J. P., Feher, G., Yeates, T. O., Komiya, H., and Rees, D. C. (1987) *Proc. Natl. Acad. Sci. USA*, **84**, 5730-5734.
3. Shuvalov, V. A., Klevanik, A. V., Sharkov, A. V., Matveetz, Yu. A., and Krukov, P. G. (1978) *FEBS Lett.*, **91**, 135-139.
4. Lauterwasser, C., Finkele, U., Scheer, H., and Zinth, W. (1991) *Chem. Phys. Lett.*, **183**, 471-477.
5. Arlt, T., Schmidt, S., Kaiser, W., Lauterwasser, C., Meyer, M., Scheer, H., and Zinth, W. (1993) *Proc. Natl. Acad. Sci. USA*, **90**, 11757-11761.
6. Shkuropatov, A. Ya., and Shuvalov, V. A. (1993) *FEBS Lett.*, **322**, 168-172.
7. Schmidt, S., Arlt, T., Hamm, P., Huber, H., Nagele, T., Wachtveitl, J., Meyer, M., Scheer, H., and Zinth, W. (1994) *Chem. Phys. Lett.*, **223**, 116-120.
8. Schmidt, S., Arlt, T., Hamm, P., Huber, H., Nagele, T., Wachtveitl, J., Zinth, W., Meyer, M., and Scheer, H. (1995) *Spectrochim. Acta. Pt. A*, **51**, 1565-1578.
9. Arlt, T., Dohse, B., Schmidt, S., Wachtveitl, J., Laussermair, E., Zinth, W., and Oesterhelt, D. (1996) *Biochemistry*, **35**, 9235-9244.
10. Holzwarth, A. R., and Muller, M. G. (1996) *Biochemistry*, **35**, 11820-11831.
11. Van Stokkum, I. H. M., Beekman, L. M. P., Jones, M. R., van Brederode, M. E., and van Grondelle, R. (1997) *Biochemistry*, **36**, 11360-11368.
12. Kennis, J. T. M., Shkuropatov, A. Ya., van Stokkum, I. H. M., Gast, P., Hoff, A. J., Shuvalov, V. A., and Aartsma, T. J. (1997) *Biochemistry*, **36**, 16231-16238.
13. Sporlein, S., Zinth, W., and Wachtveitl, J. (1998) *J. Phys. Chem. B*, **102**, 7492-7496.
14. Sporlein, S., Zinth, W., Meyer, M., Scheer, H., and Wachtveit, J. (2000) *Chem. Phys. Lett.*, **322**, 454-464.
15. Fajer, J., Brune, D. C., Davis, M. S., Forman, A., and Spaulding, L. D. (1975) *Proc. Natl. Acad. Sci. USA*, **72**, 4956-4960.
16. Kirmaier, C., and Holten, D. (1993) in *The Photosynthetic Reaction Center* (Deisenhofer, J., and Norris, J., eds.) Academic Press, San Diego, pp. 49-70.
17. Woodbury, N. W., and Allen, J. P. (1995) in *Anoxygenic Photosynthetic Bacteria* (Blankenship, R. E., Madigan, M. T., and Bauer, C. E., eds.) Kluwer Academic Publishers, Dordrecht, pp. 527-557.

18. Shuvalov, V. A., and Yakovlev, A. G. (2003) *FEBS Lett.*, **540**, 26-34.
19. Ermler, U., Fritzsch, G., Buchanan, S. K., and Michel, H. (1994) *Structure*, **2**, 925-936.
20. Deisenhofer, J., Epp, O., Sinning, I., and Michel, H. (1995) *Mol. Biol.*, **246**, 429-457.
21. Stowell, M. H. B., McPhillips, T. M., Rees, D. C., Soltis, S. M., Abresch, E., and Feher, G. (1997) *Science*, **276**, 812-816.
22. Feick, R., Shiozawa, J. A., and Ertlmaier, A. (1995) in *Anoxygenic Photosynthetic Bacteria* (Blankenship, R. E., Madigan, M. T., and Bauer, C. E., eds.) Kluwer Academic Publishers, Dordrecht, The Netherlands, pp. 699-708.
23. Bruce, B. D., Fuller, R. C., and Blankenship, R. E. (1982) *Proc. Natl. Acad. Sci. USA*, **79**, 6532-6536.
24. Kirmaier, C., Holten, D., Feick, R., and Blankenship, R. E. (1983) *FEBS Lett.*, **158**, 73-78.
25. Kirmaier, C., Blankenship, R. E., and Holten, D. (1986) *Biochim. Biophys. Acta*, **850**, 275-285.
26. Blankenship, R. E., Feick, R., Bruce, B. D., Kirmaier, C., Holten, D., and Fuller, R. C. (1983) *J. Cell. Biochem.*, **22**, 251-261.
27. Vasmel, H., and Amesz, J. (1983) *Biochim. Biophys. Acta*, **724**, 118-122.
28. Hale, M. B., Blankenship, R. E., and Fuller, R. C. (1983) *Biochim. Biophys. Acta*, **723**, 376-382.
29. Venturoli, G., Trotta, M., Feick, R., Melandri, B. A., and Zannoni, D. (1991) *Eur. J. Biochem.*, **202**, 625-634.
30. Ovchinnikov, Yu. A., Abdulaev, N. G., Zolotarev, A. S., Shmuckler, B. E., Zargarov, A. A., Kutuzov, M. A., Telezhinskaya, I. N., and Levina, N. B. (1988) *FEBS Lett.*, **231**, 237-242.
31. Ovchinnikov, Yu. A., Abdulaev, N. G., Shmuckler, B. E., Zargarov, A. A., Kutuzov, M. A., Telezhinskaya, I. N., Levina, N. B., and Zolotarev, A. S. (1988) *FEBS Lett.*, **232**, 364-368.
32. Shiozawa, J. A., Lottspeich, F., Oesterhelt, D., and Feick, R. (1989) *Eur. J. Biochem.*, **180**, 75-84.
33. Vasmel, H., Meiburg, R. F., Kramer, H. J. M., de Vos, L. J., and Amesz, J. (1983) *Biochim. Biophys. Acta*, **724**, 333-339.
34. Parot, P., Delmas, N., Garcia, D., and Vermeglio, A. (1985) *Biochim. Biophys. Acta*, **809**, 137-140.
35. Shuvalov, V. A., Shkuropatov, A. Ya., Kulakova, S. M., Ismailov, M. A., and Shkuropatova, V. A. (1986) *Biochim. Biophys. Acta*, **849**, 337-346.
36. Vasmel, H., Amesz, J., and Hoff, A. J. (1986) *Biochim. Biophys. Acta*, **852**, 159-168.
37. Scherer, P. O. J., and Fischer, S. F. (1987) *Biochim. Biophys. Acta*, **891**, 157-164.
38. Pierson, B. K., and Thornber, J. P. (1983) *Proc. Natl. Acad. Sci. USA*, **80**, 80-84.
39. Becker, M., Nagarajan, V., Middendorf, D., Parson, W. W., Martin, J. E., and Blankenship, R. E. (1991) *Biochim. Biophys. Acta*, **1057**, 299-312.
40. Feick, R., Martin, J.-L., Breton, J., Volk, M., Scheidel, G., Langenbacher, T., Urbano, C., Ogrodnik, A., and Michel-Beyerle, M. E. (1990) in *Reaction Centers of Photosynthetic Bacteria* (Michel-Beyerle, M. E., ed.) Springer-Verlag, Berlin, pp. 181-188.
41. Volk, M., Scheidel, G., Ogrodnik, A., Feick, R., and Michel-Beyerle, M. E. (1991) *Biochim. Biophys. Acta*, **1058**, 217-224.
42. Wachtveitl, J., Huber, H., Feick, R., Rautter, J., Muh, F., and Lubitz, W. (1998) *Spectrochim. Acta. Pt. A*, **54**, 1231-1245.
43. Vos, M. H., Lambry, J.-C., Robles, S. J., Youvan, D. C., Breton, J., and Martin, J.-L. (1991) *Proc. Natl. Acad. Sci. USA*, **88**, 8885-8889.
44. Vos, M. H., Rappaport, F., Lambry, J.-C., Breton, J., and Martin, J.-L. (1993) *Nature*, **363**, 320-325.
45. Vos, M. H., Jones, M. R., Hunter, C. N., Breton, J., Lambry, J.-C., and Martin, J.-L. (1994) *Biochemistry*, **33**, 6750-6757.
46. Vos, M. H., Jones, M. R., Breton, J., Lambry, J.-C., and Martin, J.-L. (1996) *Biochemistry*, **35**, 2687-2692.
47. Stanley, R. J., and Boxer, S. G. (1995) *J. Phys. Chem.*, **99**, 859-863.
48. Streltsov, A. M., Yakovlev, A. G., Shkuropatov, A. Ya., and Shuvalov, V. A. (1996) *FEBS Lett.*, **383**, 129-132.
49. Streltsov, A. M., Vulto, S. I. E., Shkuropatov, A. Ya., Hoff, A. J., Aartsma, T. J., and Shuvalov, V. A. (1998) *J. Phys. Chem. B*, **102**, 7293-7298.
50. Yakovlev, A. G., Shkuropatov, A. Ya., and Shuvalov, V. A. (2000) *FEBS Lett.*, **466**, 209-212.
51. Yakovlev, A. G., and Shuvalov, V. A. (2000) *J. Chin. Chem. Soc.*, **47**, 709-714.
52. Yakovlev, A. G., Shkuropatov, A. Ya., and Shuvalov, V. A. (2002) *Biochemistry*, **41**, 2667-2674.
53. Yakovlev, A. G., Shkuropatov, A. Ya., and Shuvalov, V. A. (2002) *Biochemistry*, **41**, 14019-14027.
54. Streltsov, A. M., Aartsma, T. J., Hoff, A. J., and Shuvalov, V. A. (1997) *Chem. Phys. Lett.*, **266**, 347-352.
55. Vos, M. H., Rischel, C., Jones, M. R., and Martin, J.-L. (2000) *Biochemistry*, **39**, 8353-8361.
56. Yakovlev, A. G., Vasilieva, L. G., Shkuropatov, A. Ya., Bolgarina, T. I., Shkuropatova, V. A., and Shuvalov, V. A. (2003) *J. Phys. Chem. A*, **107**, 8330-8338.
57. Potter, J. A., Fyfe, P. K., Frolov, D., Wakeham, M. C., van Grondelle, R., Robert, B., and Jones, M. R. (2005) *J. Biol. Chem.*, **280**, 27155-27164.
58. Yakovlev, A. G., Jones, M. R., Potter, J. A., Vasilieva, L. G., Shkuropatov, A. Y., and Shuvalov, V. A. (2005) *Chem. Phys.*, **319**, 297-307.
59. Fyfe, P. K., Ridge, J. P., McAuley, K. E., Cogdell, R. J., Isaacs, N. W., and Jones, M. R. (2000) *Biochemistry*, **39**, 5953-5960.
60. Williams, J. C., Alden, R. G., Murchison, H. A., Peloquin, J. M., Woodbury, N. W., and Allen, J. P. (1992) *Biochemistry*, **31**, 11029-11037.
61. Shuvalov, V. A., Shkuropatov, A. Ya., Kulakova, S. M., Ismailov, M. A., and Shkuropatova, V. A. (1986) *Biochim. Biophys. Acta*, **849**, 337-348.
62. Fok, M. B., and Borisov, A. Yu. (1981) *Mol. Biol.* (Moscow), **15**, 575-581.
63. Noks, P. P., Kononenko, A. A., and Rubin, A. B. (1979) *Bioorg. Khim.*, **5**, 879-885.
64. Heller, B. A., Holten, D., and Kirmaier, C. (1995) *Science*, **269**, 940-945.
65. Schenk, C. C., Parson, W. W., Holten, D., and Windsor, M. W. (1981) *Biochim. Biophys. Acta*, **635**, 383-392.
66. Breton, J., Martin, J.-L., Lambry, J. C., Robles, S. J., and Youvan, D. C. (1990) in *Reaction Centers of Photosynthetic Bacteria* (Michel-Beyerle, M. E., ed.) Springer Series in Biophysics, Pt. 6, Springer, New York, pp. 293-302.

67. Shuvalov, V. A., Shkuropatov, A. Ya., and Klevanik, A. V. (1992) in *The Photosynthetic Bacterial Reaction Center II: Structure*, *Spectroscopy*, *and Dynamics* (Breton, J., and Vermeglio, A., eds.) Plenum Press, New York-London, pp. 245-253.
68. Eberl, U., Gilbert, M., Keupp, W., Langenbacher, T., Siegl, J., Sinning, I., Ogrodnik, A., Robles, S. J., Breton, J., Yovan, D. C., and Michel-Beyerle, M. E. (1992) in *The Photosynthetic Bacterial Reaction Center II: Structure*, *Spectroscopy*, *and Dynamics* (Breton, J., and Vermeglio, A., eds.) Plenum Press, New York-London, pp. 253-262.
69. Plato, M., Lendzian, F., Lubitz, W., Trankle, E., and Mobius, K. (1988) in *The Photosynthetic Bacterial Reaction Center: Structure and Dynamics* (Breton, J., and Vermeglio, A., eds.) Plenum Press, New York-London, pp. 379-388.
70. De Rege, P. J. F., Williams, S. A., and Therien, M. J. (1995) *Science*, **269**, 1409-1413.
71. Marcus, R. A. (1988) in *The Photosynthetic Bacterial Reaction Center: Structure and Dynamics* (Breton, J., and Vermeglio, A., eds.) Plenum Press, New York-London, pp. 389-398.
72. Bixon, M., and Jortner, J. (1986) *J. Phys. Chem.*, **90**, 3795-3800.
73. Kitzing, E., and Kuhn, H. (1990) *J. Phys. Chem.*, **94**, 1699-1702.
74. Parson, W. W., and Warshel, A. (1987) *J. Am. Chem. Soc.*, **109**, 6152-6163.
75. Fleming, G. R., Martin, J.-L., and Breton, J. (1988) *Nature*, **333**, 190-192.
76. Larsson, S., and Ivashin, N. V. (1999) *J. Appl. Spectrosc.*, **66**, 539-543.
77. Bixon, M., Jortner, J., Plato, M., and Michel-Beyerle, M. E. (1988) in *The Photosynthetic Bacterial Reaction Center: Structure and Dynamics* (Breton, J., and Vermeglio, A., eds.) Plenum Press, New York-London, pp. 399-419.